Vehicle Safety of the Velocity Obstacle Algorithm

Aurora Haraldsen[1], Martin S. Wiig[2] and Kristin Y. Pettersen[1,2]

Abstract— This paper presents a mathematical analysis of the velocity obstacle algorithm applied to a nonholonomic vehicle for avoiding a moving obstacle in the plane. The velocity obstacle algorithm can be used for local navigation among dynamic obstacles by continually computing a set of unsafe velocities, and avoid the velocities inside of this set. The method is commonly used for reactive collision avoidance as it requires only limited knowledge of the obstacle behaviour and is computationally inexpensive. A drawback of previous analyses is the assumption that the vehicle and the obstacle are constrained to follow specific types of paths, or the velocities are assumed constant. We analyze the algorithm without such constraints and derive a set of conditions to prove that vehicle safety can be guaranteed in the general case. Moreover, we prove that the method can safely be applied to vehicles subject to nonholonomic constraints, with limited turning rates.

I. INTRODUCTION

Autonomous vehicles present a large potential for scientific and commercial applications. To achieve autonomous or semi-autonomous operations, the capability to avoid static and dynamic obstacles without human intervention is crucial for mission success and vehicle safety. Reactive collision avoidance is important in autonomous operations when motion planning algorithms fall short. In complex environments with dynamic obstacles the vehicle has to react quickly, which can make the time consumption of motion planning algorithms unacceptable. Moreover, reactive algorithms adapt far better to environments with unexpected changes. Hence, there is a need for reactive collision avoidance algorithms for avoiding moving obstacles.

A common approach to reactive collision avoidance in dynamic environments is the velocity obstacle (VO) approach [1], where obstacles are represented as cones in the velocity space. The cones, called velocity obstacles, represent the set of constant velocities causing a collision between the vehicle and an obstacle at some future time. Maintaining velocities outside of the set guarantees a collision-free trajectory of the vehicle. Navigation among multiple moving obstacles is possible by avoiding the velocities inside the union of all individual velocity obstacles. The concept can be applied in motion planning algorithms by searching over a tree of successive, feasible maneuvers [1].

The velocity obstacle approach has been extended to include kinematic and dynamic vehicle constraints in [2], [3], and has been used to implement the International regulations for preventing collisions at sea (COLREGS) [4], [5]. The

acceleration-velocity obstacles (AVO) [6] accounts for constraints in the vehicle's acceleration. Other methods, such as the nonlinear velocity obstacle [7] focus mainly on capturing the behaviour of the obstacle rather than the constraints on the vehicle. The velocity obstacle algorithm is extended to 3D in [8], [9] where the 3D velocity space is divided into a set of discrete planes, and the 2D velocity obstacle is applied to each plane.

Many examples of reactive collision avoidance in decentralized, multi-agent systems employ velocity obstacles [6], [10], [11], [12], [13]. To avoid oscillations, the reactive behaviour of other agents must be taken into account, by implicitly assuming that the other agents make the similar collision avoidance reasoning. Several approaches are then able to provide strong proofs of agent safety [10], [12].

Velocity obstacles have been successfully applied to nonholonomic systems. However, the theoretical foundation of the algorithm applied to such systems needs to be expanded. Furthermore, safety should be investigated in combination with the vehicle's nominal behaviour, such as reaching a target or path following. In this paper, we present a mathematical analysis of the velocity obstacle algorithm applied to a vehicle that is subject to nonholonomic constraints, for avoiding a moving obstacle that is capable of both turning and accelerating towards the vehicle at any point in time. We provide analytical proof of vehicle safety in the presence of the obstacle, while also guaranteeing that the vehicle will reach its target. We make very few assumptions on the obstacle behaviour. Instead, we assume that the vehicle's forward speed and turning rate are lower bounded by realistic minimum values. The lower bound on the vehicle's turning rate is especially interesting, because it guarantees safety of the vehicle even when the turning rate is limited. Motivated by [14], the vehicle's forward speed is decoupled from its heading, by requiring the vehicle to maintain a constant forward speed, and only controlling the turning rate. Thus, the algorithm is also suitable for vehicles that are restricted by heavy linear acceleration constraints, and vehicles with limited speed envelopes.

The paper is organized as follows. Section II describes the vehicle model and associated control system, and the model used to describe a moving obstacle. In Section III the collision avoidance algorithm is presented. The algorithm is mathematically analyzed in Section IV, supported by numerical simulations in Section V. The concluding remarks are given in Section VI.

---

[1]Centre for Autonomous Marine Operations and Systems (NTNU AMOS), Department of Engineering Cybernetics, Norwegian University of Science and Technology, NO-7491 Trondheim, Norway.

[2]Norwegian Defence Research Establishment (FFI), P.O. Box 25, N-2027 Kjeller, Norway.

II. SYSTEM DESCRIPTION

In this section we describe the system consisting of a vehicle and a moving obstacle. We present the vehicle model in Section II-A, and the obstacle model in Section II-B. The vehicle's control objective is stated in Section II-C, where we require the vehicle to move towards a target while keeping a minimum safety distance to the obstacle. The target reaching guidance law is stated in Section II-D, and the kinematic heading controller is stated in Section II-E.

A. Vehicle model

The vehicle is modeled as a kinematic unicycle-type vehicle:

$$
\begin{aligned}
\dot{x}(t) &= u \cos(\psi(t)), \\
\dot{y}(t) &= u \sin(\psi(t)), \\
\dot{\psi}(t) &= r(t),
\end{aligned}
\tag{1}
$$

where $\boldsymbol{p}(t) \triangleq [x(t), y(t)]^\top$ are the Cartesian coordinates of the vehicle, u is the forward speed, and $\psi(t)$ and $r(t)$ are the heading and heading rate, respectively. The vehicle's velocity vector is denoted $\boldsymbol{v}(t) \triangleq [\dot{x}(t), \dot{y}(t)]^\top$.

For convenience, we assume that the vehicle maintains a constant forward speed given by an arbitrary outer-loop controller, but directly controls the turning rate, $r(t)$, in order to follow the heading reference generated by the control system:

Assumption 1: The vehicle's forward speed $u > 0$ is constant.

Assumption 2: The vehicle's heading rate, $r(t)$, is directly controlled and bounded by

$$
|r(t)| \le r_{\max},
\tag{2}
$$

where $r_{\max} > 0$ is a constant parameter.

B. Obstacle model

The obstacle is modeled as a nonholonomic vehicle:

$$
\begin{aligned}
\dot{x}_{\mathrm{o}}(t) &= u_{\mathrm{o}}(t) \cos(\psi_{\mathrm{o}}(t)), \\
\dot{y}_{\mathrm{o}}(t) &= u_{\mathrm{o}}(t) \sin(\psi_{\mathrm{o}}(t)), \\
\dot{\psi}_{\mathrm{o}}(t) &= r_{\mathrm{o}}(t), \\
\dot{u}_{\mathrm{o}}(t) &= a_{\mathrm{o}}(t),
\end{aligned}
\tag{3}
$$

where $\boldsymbol{p}_{\mathrm{o}}(t) \triangleq [x_{\mathrm{o}}(t), y_{\mathrm{o}}(t)]^\top$ are the Cartesian coordinates of the obstacle center, $u_{\mathrm{o}}(t)$ and $a_{\mathrm{o}}(t)$ are the forward speed and acceleration, and $\psi_{\mathrm{o}}(t)$ and $r_{\mathrm{o}}(t)$ are the heading and heading rate, respectively. The obstacle's velocity vector is denoted $\boldsymbol{v}_o(t) \triangleq [\dot{x}_{\mathrm{o}}(t), \dot{y}_{\mathrm{o}}(t)]^\top$.

Assumption 3: The obstacle can be modeled as a moving, circular domain $\mathcal{D}_{\mathrm{o}}$ with radius $R_{\mathrm{o}} > 0$.

Assumption 4: The obstacle's heading rate, $r_{\mathrm{o}}(t)$, and forward acceleration, $a_{\mathrm{o}}(t)$, are bounded by

$$
\begin{aligned}
|r_{\mathrm{o}}(t)| &\le r_{\mathrm{o},\max}, \\
|a_{\mathrm{o}}(t)| &\le a_{\mathrm{o},\max},
\end{aligned}
\tag{4}
$$

where $r_{\mathrm{o},\max} \ge 0$ and $a_{\mathrm{o},\max} \ge 0$ are constant parameters.

Assumption 5: The obstacle's forward speed $u_{\mathrm{o}}(t) \ge 0$ is bounded by

$$
u_{\mathrm{o}}(t) \le u_{\mathrm{o},\max},
\tag{5}
$$

where $u_{\mathrm{o},\max} < u$ is a constant parameter.
By Assumption 5 we require the vehicle's speed, u, to be lower bounded by the maximum speed of the obstacle. This is in general a necessary requirement when the obstacle is non-cooperative, as it ensures that the vehicle is able to escape the obstacle at some point in time.

C. Control objective

The objective of the control system is to make the vehicle come within an acceptable distance of a target position $\boldsymbol{p}_{\mathrm{t}} \triangleq [x_{\mathrm{t}}, y_{\mathrm{t}}]^\top$ at an unspecified point in time $t_{\mathrm{f}} \in [0, \infty)$. The control objective can be written:

$$
\|\boldsymbol{p}_{\mathrm{t}} - \boldsymbol{p}(t_{\mathrm{f}})\| \le d_{\mathrm{a}},
\tag{6}
$$

where $d_{\mathrm{a}} \ge 0$ is the acceptance distance. The goal should be achieved while keeping at least a minimum safety distance, d_ϵ, to the obstacle:

$$
d(t) - R_{\mathrm{o}} \ge d_\epsilon > 0, \quad \forall t \in [t_0, t_{\mathrm{f}}],
\tag{7}
$$

where $d(t) \triangleq \|\boldsymbol{p}(t) - \boldsymbol{p}_{\mathrm{o}}(t)\|$ is the distance between the vehicle and obstacle centers.

D. Guidance law

To make the vehicle reach the target position $\boldsymbol{p}_{\mathrm{t}}$, the heading reference is generated by a pure pursuit guidance law [15]. The guidance velocity is given by

$$
\boldsymbol{v}_{\mathrm{dg}}(t) \triangleq u \frac{\boldsymbol{p}_{\mathrm{t}} - \boldsymbol{p}(t)}{\|\boldsymbol{p}_{\mathrm{t}} - \boldsymbol{p}(t)\|},
\tag{8}
$$

where $u = \|\boldsymbol{v}_{\mathrm{dg}}(t)\|$ is the speed of the vehicle. The desired heading is given by

$$
\psi_{\mathrm{dg}}(t) \triangleq \operatorname{atan2}\left(y_{\mathrm{t}} - y(t), x_{\mathrm{t}} - x(t)\right).
\tag{9}
$$

E. Heading controller

To make the vehicle turn towards the desired heading $\psi_{\mathrm{dg}}(t)$ with maximum turning power, we employ the kinematic heading controller:

$$
r(t) = \begin{cases}
0, & \text{if } \tilde{\psi}(t) = 0, \\
r_{\max}, & \text{if } \tilde{\psi}(t) = (0, \pi], \\
-r_{\max}, & \text{if } \tilde{\psi}(t) = (-\pi, 0).
\end{cases}
\tag{10}
$$

The error variable $\tilde{\psi}(t) \triangleq \psi_{\mathrm{dg}}(t) - \psi(t)$ is chosen to belong in the range $(-\pi, \pi]$ to ensure that the vehicle always takes the shortest turn towards the desired heading.

III. COLLISION AVOIDANCE ALGORITHM

In this section we describe the velocity obstacle algorithm [1]. We will give a brief introduction to the main concepts behind the algorithm, which is the basis for deciding when the vehicle is in need of collision avoidance, in Section III-A. We will formulate the specific conditions for when the vehicle should enter or exit collision avoidance (CA) mode in Section III-B. To avoid a collision with the obstacle, we propose a set of turning rules for the vehicle in Section III-C.
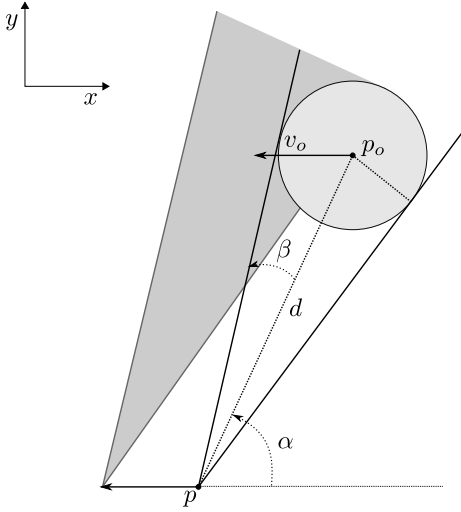
Fig. 1: The collision cone (area within the solid, tangent lines) and the velocity obstacle (shaded area).

A. The velocity obstacle

Consider Figure 1, where the vehicle is illustrated as a point mass, and the moving obstacle as a circular domain with radius R_o. The line segment going from the center of the vehicle, $\boldsymbol{p}(t)$, to the center of the obstacle, $\boldsymbol{p}_\mathrm{o}(t)$, can be described by the length $d(t)$, and the orientation $\alpha(t) \triangleq \mathrm{atan2}(y_\mathrm{o}(t) - y(t), x_\mathrm{o}(t) - x(t))$. If the obstacle is static, and the vehicle's heading angle lies between the angular boundaries $\alpha(t) \pm \sin^{-1}(R_\mathrm{o}/d(t))$, then the vehicle is headed for a collision. The condition can be directly translated to a cone in the velocity space, whose sides are rays pointing along these angular boundaries (see Figure 1). We define the ray going from $\boldsymbol{p}$, in the direction of the vector $\boldsymbol{v}$, as

$$l(\boldsymbol{p}, \boldsymbol{v}) \triangleq \{ \boldsymbol{p} + \boldsymbol{v}t \mid t \geq 0 \}.$$

For a moving obstacle, the condition can be formulated in the velocity space as the collision cone [1]:

Definition 1 (Collision cone): The set of relative velocities $\boldsymbol{v}_\mathrm{r} \triangleq \boldsymbol{v} - \boldsymbol{v}_o$ that will cause a collision between the obstacle and the vehicle, assuming the velocity vectors $\boldsymbol{v}$ and $\boldsymbol{v}_o$ are constant over time, is defined as

$$\mathcal{CC}_\mathrm{o} \triangleq \{ \boldsymbol{v}_\mathrm{r} \mid l(\boldsymbol{p}, \boldsymbol{v}_\mathrm{r}) \cap \mathcal{D}_\mathrm{o} \neq \varnothing \}. \tag{11}$$

This corresponds to any relative velocity whose ray intersects the obstacle domain $\mathcal{D}_\mathrm{o}$. The collision cone can equivalently be described in terms of absolute velocities as the velocity obstacle [1]:

Definition 2 (Velocity obstacle): The set of absolute velocities $\boldsymbol{v}$ that will cause a collision between the obstacle and the vehicle, assuming the velocity vectors $\boldsymbol{v}$ and $\boldsymbol{v}_o$ are constant over time, is defined as

$$\mathcal{VO}_\mathrm{o} \triangleq \mathcal{CC}_\mathrm{o} \oplus \boldsymbol{v}_o, \tag{12}$$

where the operator $\oplus$ denotes the Minkowski sum.
The formulation is equivalent to translating the collision cone by the obstacle velocity, $\boldsymbol{v}_o$, as seen in Figure 1.

Recall that in Section II-C we required the vehicle to maintain at least a safety distance, d_ϵ, to the obstacle. The

safety distance is necessary in order to compensate for the area of the vehicle, allowing the vehicle to be considered as a point mass. The safety distance can be chosen large enough to also compensate for any required separation distance between the vehicle and the obstacle. Since the tangents of the collision cone are determined by the radius of the obstacle, we simply extend the obstacle radius by d_ϵ to account for the additional distance. We will denote the extended radius as $R_{\mathrm{o}|\epsilon} \triangleq R_\mathrm{o} + d_\epsilon$. The collision cone can then be computed for the extended obstacle domain, $\mathcal{D}_{\mathrm{o}|\epsilon}$. The tangents of the (extended) collision cone will be denoted as

$$\psi_\mathrm{t}^{\pm}(t) \triangleq \alpha(t) \pm \beta(t), \tag{13}$$

where we use the superscript $\pm$ to distinguish between the two angles, and

$$\beta(t) \triangleq \sin^{-1}\left(\frac{R_\mathrm{o} + d_\epsilon}{d(t)} \right). \tag{14}$$

Moreover, we will denote the collision cone and the velocity obstacle for the extended obstacle domain as $\mathcal{CC}_{\mathrm{o}|\epsilon}$ and $\mathcal{VO}_{\mathrm{o}|\epsilon}$, respectively.

B. Switching conditions

The velocity obstacle can be used to decide if the vehicle is headed for a collision with the obstacle. Unlike the original VO method [1] which employs a time-horizon to distinguish between obstacles with imminent collision and long time to collision, we will decide when the vehicle should switch to collision avoidance mode based on the distance between the obstacle and the vehicle, motivated by [14].

The control system is switched to collision avoidance mode at a time $t_1 \geq t_0$ when the obstacle is within a specified threshold distance of the vehicle, simultaneously as the guidance velocity is unsafe:

$$\begin{aligned} d(t_1) &\leq d_\mathrm{threshold}, \\ \boldsymbol{v}_\mathrm{dg}(t_1) &\in \mathcal{VO}_{\mathrm{o}|\epsilon}(t_1), \end{aligned} \tag{15}$$

where $d_\mathrm{threshold} > 0$ is a constant design parameter. The vehicle exits collision avoidance mode at a time $t_2 > t_1$ when the guidance velocity is safe:

$$\boldsymbol{v}_\mathrm{dg}(t_2) \notin \mathcal{VO}_{\mathrm{o}|\epsilon}(t_2). \tag{16}$$

C. The avoidance maneuver

If the vehicle enters collision avoidance mode the vehicle is currently maintaining an unsafe velocity. The vehicle should then perform an avoidance maneuver in order to avoid a possible collision. In order to formulate the turning rules for the avoidance maneuver we must first introduce some mathematical notation.

Motivated by [10], the vehicle is said to be in a conflict with the obstacle if its relative heading angle with respect to the obstacle, defined as

$$\psi_\mathrm{r}(t) \triangleq \mathrm{atan2}(\dot{y}(t) - \dot{y}_\mathrm{o}(t), \dot{x}(t) - \dot{x}_\mathrm{o}(t)), \tag{17}$$
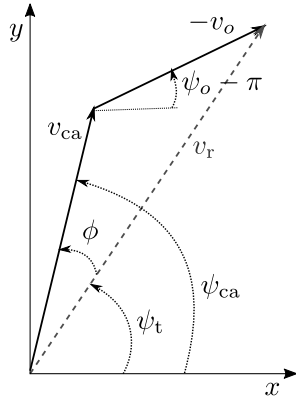
Fig. 2: The heading angles $\psi_{\text{ca}}^{\pm}$ can be found geometrically by the computation of $\phi^{\pm}$.

lies between the angular boundaries of the collision cone defined in (13), i.e. $\psi_{\text{r}}(t) \in \left(\psi_{\text{t}}^{-}(t), \psi_{\text{t}}^{+}(t)\right)$. This can equivalently be described by the following definition:

Definition 3 (Conflict): A conflict occurs between the vehicle and the obstacle if the vehicle, with zero control input $r(t) = 0$, will violate condition (7) at some point in the future, provided the obstacle maintains its current velocity:

$$|\psi_{\text{r}}(t) - \alpha(t)| < \beta(t). \tag{18}$$

Since we generally want to work with absolute velocities, it can be convenient to express a conflict in terms of the absolute heading of the vehicle. The heading angles corresponding to the tangents $\psi_{\text{t}}^{\pm}(t)$ can be found geometrically by considering Figure 2, as

$$\psi_{\text{ca}}^{\pm}(t) \triangleq \phi^{\pm}(t) + \psi_{\text{t}}^{\pm}(t), \tag{19}$$

where the angles $\phi^{\pm}(t)$ can be computed by using the Law of Sines on the triangle consisting of $\boldsymbol{v}_{\text{ca}}$, $\boldsymbol{v}_o$ and $\boldsymbol{v}_{\text{r}}$, as

$$\phi^{\pm}(t) = \sin^{-1}\left(\frac{u_{\text{o}}(t)}{u}\sin(\pi + \psi_{\text{t}}^{\pm}(t) - \psi_{\text{o}}(t))\right). \tag{20}$$

Based on [10], a measure of the distances to a conflict can then be found as

$$\gamma^{\pm}(t) \triangleq \pm\psi(t) \mp \psi_{\text{ca}}^{\pm}(t), \tag{21}$$

where the angles $\gamma^{\pm}(t)$ are wrapped into the domain $(-2\pi, 2\pi]$ such that the distances are negative when the vehicle is in a conflict, and positive otherwise. The angles correspond to the angular distances the vehicle must turn to enter (or exit) a conflict in both directions. The shortest angular distance to a conflict, denoted $\gamma(t)$, is defined as

$$\gamma(t) \triangleq \begin{cases} \gamma^{+}(t), & \text{if } \psi_{\text{r}}(t) - \alpha(t) \geq 0, \\ \gamma^{-}(t), & \text{if } \psi_{\text{r}}(t) - \alpha(t) < 0, \end{cases} \tag{22}$$

where the angular difference is mapped to the domain $\left(\psi_{\text{r}}(t) - \alpha(t)\right) \in (-\pi, \pi]$.

We are now ready to present the structure of the avoidance maneuver, where we need to consider two different scenarios. In the first scenario, the angular distances to a conflict, $\gamma^{\pm}(t)$, are negative, and a conflict then arises when the distance, $d(t)$, is reduced to $d_{\text{threshold}}$. In the second scenario, the angular distance to a conflict reaches zero while $d(t) <$

$d_{\text{threshold}}$. In the first case, the vehicle can turn in either direction to exit the conflict safely as long as $d_{\text{threshold}}$ is chosen with this in mind. The avoidance maneuver is then given by the following turning rule, which will make the vehicle seek to pass behind the obstacle. This is obtained by maximizing the difference between the obstacle heading and the heading candidates defined in (19), as presented in [14]:

$$\begin{aligned} d(t) &= d_{\text{threshold}}, \\ j &= \arg\max_{j=\pm}|\psi_{\text{o}}(t) - \psi_{\text{ca}}^{j}(t)|, \end{aligned} \tag{23}$$

where j is the turning parameter, and the angular difference is mapped into the interval $(-\pi, \pi]$. The control input is given by

$$r(t) = \begin{cases} r_{\max}, & \text{if } j = + \mid \gamma^{+}(t) \leq \epsilon, \\ -r_{\max}, & \text{if } j = - \mid \gamma^{-}(t) \leq \epsilon. \end{cases} \tag{24}$$

In the second case, the vehicle can only turn safely in one direction, i.e. away from the nearest conflict. We then let the avoidance maneuver be defined as

$$d(t) < d_{\text{threshold}},$$

$$r(t) = \begin{cases} r_{\max}, & \text{if } \gamma(t) = \gamma^{+}(t) \mid \gamma^{+}(t) \leq \epsilon, \\ -r_{\max}, & \text{if } \gamma(t) = \gamma^{-}(t) \mid \gamma^{-}(t) \leq \epsilon. \end{cases} \tag{25}$$

In both cases, the vehicle will turn until it is a constant, angular safety distance $\epsilon \geq 0$ away from a conflict.

IV. MATHEMATICAL ANALYSIS

In this section, we present a mathematical analysis of the collision avoidance algorithm stated in Section III, applied to the system described in Section II. In particular, we will prove that the vehicle modeled by (1), following the reference generated by the guidance law and the CA algorithm, will reach the target position while keeping at least a safety distance from an obstacle described by (3), provided that all stated assumptions hold.

In Lemma 1 and 2 we prove that the distance between the vehicle and the obstacle, $d(t) - R_o$, cannot be reduced to less than d_ϵ, provided the vehicle never enters a conflict with the obstacle. To make Lemma 2 useful, we derive a necessary bound on vehicle's turning rate in Theorem 1, in order to prove that the vehicle will avoid a conflict with the obstacle if the vehicle starts outside a conflict, and continuously turns away from the conflict at maximum turning rate. Finally, in Theorem 2 we prove safety of the overall system, allowing the vehicle to enter a conflict with the obstacle under the requirement that the vehicle and obstacle are initially separated by a minimum distance.

Lemma 1: Consider a static obstacle, and let the vehicle and the obstacle initially be separated by a distance $d(t_0) > R_{\text{o}|\epsilon}$. If the vehicle maintains a heading angle satisfying

$$|\psi(t) - \alpha(t)| = \beta(t), \quad \forall t \geq t_0, \tag{26}$$

where $\beta(t)$ is given by (14), then the vehicle will converge to a circle with radius $R_{\text{o}|\epsilon}$ and center in the obstacle center, $\boldsymbol{p}_{\text{o}}$. Moreover, if the vehicle maintains a heading angle satisfying

$$|\psi(t) - \alpha(t)| \geq \beta(t), \quad \forall t \geq t_0, \tag{27}$$

then
$$d(t) - R_o \geq d_\epsilon, \quad \forall t \geq t_0. \tag{28}$$

Proof: Consider the line segment going from the origin of the vehicle, $\boldsymbol{p}(t)$, to the origin of the obstacle, $\boldsymbol{p}_o$, with length $d(t)$ and orientation $\alpha(t)$. The time-derivative of $d(t)$ is found geometrically as

$$\dot{d}(t) = -u\cos(\psi(t) - \alpha(t)). \tag{29}$$

Let the vehicle satisfy (26) where $\beta(t)$ is defined in (14). We can then write (29) as

$$\dot{d}(t) = -u\sqrt{1 - \left(\frac{R_{o|\epsilon}}{d(t)}\right)^2}. \tag{30}$$

Solving (30) for $d(t)$, it can be seen that $d(t)$ has a minimum value equal to $R_{o|\epsilon}$, when $\dot{d}(t) = 0$. Hence, we have established that $d(t)$ is lower bounded by $R_{o|\epsilon}$. Since the vehicle initially satisfies $d(t_0) > R_{o|\epsilon}$, then by (30) $\dot{d}(t_0) < 0$. Moreover, $\dot{d}(t) < 0 \; \forall d(t) > R_{o|\epsilon}$, and $\dot{d}(t) = 0$ if and only if $d(t) = R_{o|\epsilon}$. Thus, $\dot{d}(t) \leq 0 \; \forall t \geq t_0$. Since $\dot{d}(t) \leq 0$ and $d(t)$ is lower bounded, then $d(t) \to R_{o|\epsilon}$ as $t \to \infty$. Hence, the position of the vehicle, $\boldsymbol{p}(t)$, converges to a circle with radius $R_{o|\epsilon}$ and center in $\boldsymbol{p}_o$.

Now, let the vehicle satisfy (27). The time-derivative of $d(t)$ from (29) then satisfies

$$\dot{d}(t) \geq -u\sqrt{1 - \left(\frac{R_{o|\epsilon}}{d(t)}\right)^2}. \tag{31}$$

Hence,

$$d(t) - R_o \geq d_\epsilon, \quad \forall t \geq t_0, \tag{32}$$

which concludes the proof. $\blacksquare$

Lemma 2: Consider an obstacle moving with time-varying velocity $\boldsymbol{v}_o(t)$, and let the vehicle and the obstacle initially be separated by a distance $d(t_0) > R_{o|\epsilon}$. If the vehicle maintains a heading angle satisfying

$$|\psi_r(t) - \alpha(t)| \geq \beta(t), \quad \forall t \geq t_0, \tag{33}$$

then

$$d(t) - R_o \geq d_\epsilon, \quad \forall t \geq t_0. \tag{34}$$

Proof: Consider a coordinate frame n_o attached to the obstacle and aligned with the inertial frame n, moving with the obstacle velocity $\boldsymbol{v}_o(t)$. In this frame, the obstacle is static and the vehicle has the velocity $\boldsymbol{v}_r(t) = \boldsymbol{v}(t) - \boldsymbol{v}_o(t)$. Hence, Lemma 1 can be applied for the vehicle with the relative velocity $\boldsymbol{v}_r(t)$ and heading $\psi_r(t) = \angle\boldsymbol{v}(t) - \boldsymbol{v}_o(t)$ defined in (17). $\blacksquare$

The above analysis supports the main concept behind the algorithm, which serves as a useful metric to decide if the vehicle should change its course at a point in time. We will apply Lemma 2 in the following analysis, where we consider the full system described in Section II, in combination with the collision avoidance algorithm stated in Section III.

Theorem 1: Consider an obstacle described by (3) and a vehicle described by (1). If Assumption 1-5 hold, and the vehicle starts outside a conflict, i.e.:

$$|\psi_r(t_0) - \alpha(t_0)| \geq \beta(t_0), \tag{35}$$

then the vehicle will maintain a distance to the obstacle satisfying

$$d(t) - R_o \geq d_\epsilon, \quad \forall t \geq t_0, \tag{36}$$

provided it maintains a continuous control input, $r(t)$, satisfying

$$\begin{aligned}\gamma^+(t) = 0 &\implies r(t) = r_{\max}, \\ \gamma^-(t) = 0 &\implies r(t) = -r_{\max},\end{aligned} \tag{37}$$

where

$$r_{\max} \geq r_{o,\max}\frac{u_{o,\max}}{u} + \frac{a_{o,\max}}{\sqrt{u^2 - u_{o,\max}^2}}. \tag{38}$$

Proof: The proof of this theorem follows along the lines of the proof presented in [10], which argues that if the vehicle starts conflict-free, and continuously turns away from the conflict or exerts no control input $r(t) = 0$, then the vehicle avoids a collision with another vehicle following the same collision avoidance algorithm. Since we are not dealing with a cooperating vehicle but rather with an unpredictable obstacle, an extended analysis is required, and we also end up with a necessary bound on the vehicle's turning rate.

The angular distances to a conflict, $\gamma^\pm$, can be found from substituting (13) and (19) into (21) as

$$\gamma^\pm = \pm\psi \mp (\alpha \pm \beta + \phi^\pm), \tag{39}$$

which has the time-derivative

$$\frac{d\gamma^\pm}{dt} = \pm r \mp \left(\frac{d\alpha}{dt} \pm \frac{d\beta}{dt}\right) \mp \frac{d\phi^\pm}{dt}. \tag{40}$$

The time-derivative of α is found geometrically as

$$\frac{d\alpha}{dt} = -\frac{\|\boldsymbol{v}_r\|}{d}\sin(\psi_r - \alpha), \tag{41}$$

while the time-derivative of β can be computed from (14) as

$$\frac{d\beta}{dt} = \frac{d}{dt}\left(\sin^{-1}\left(\frac{R_{o|\epsilon}}{d}\right)\right) \tag{42}$$

$$= -\dot{d}\frac{R_{o|\epsilon}}{d\sqrt{d^2 - (R_{o|\epsilon})^2}} \tag{43}$$

$$= \frac{\|\boldsymbol{v}_r\|}{d}\cos(\psi_r - \alpha)\tan(\beta), \tag{44}$$

where $\dot{d}$ is found geometrically. The time-derivative of $\phi^\pm$ can be computed from (20) as

$$\frac{d\phi^\pm}{dt} = \frac{d\left(\psi_{o,-}^\pm\right)}{dt} \cdot \frac{\partial\phi^\pm}{\partial\psi_{o,-}^\pm} + \frac{d\left(u_o\right)}{dt} \cdot \frac{\partial\phi^\pm}{\partial u_o}, \tag{45}$$

where we define $\psi_{o,-}^\pm \triangleq \pi + \psi_t^\pm - \psi_o$. We compute the terms as

$$\frac{d\left(\psi_{o,-}^\pm\right)}{dt} \cdot \frac{\partial\phi^\pm}{\partial\psi_{o,-}^\pm} = \tag{46}$$

$$= \frac{\partial}{\partial\psi_{o,-}^\pm}\left(\sin^{-1}\left(\frac{u_o\sin(\psi_{o,-}^\pm)}{u}\right)\right)\dot{\psi}_{o,-}^\pm \tag{47}$$

$$= \left(-r_o + \frac{d\alpha}{dt} \pm \frac{d\beta}{dt}\right)\frac{(u_o/u)\cos(\psi_{o,-}^\pm)}{\sqrt{1 - (u_o/u)^2\sin^2(\psi_{o,-}^\pm)}}, \tag{48}$$

and

$$\frac{d(u_o)}{dt} \cdot \frac{\partial \phi^\pm}{\partial u_o} = \tag{49}$$

$$= \frac{\partial}{\partial u_o}\left(\sin^{-1}\left(\frac{u_o \sin(\psi_{o,-}^\pm)}{u}\right)\right)\dot{u}_o \tag{50}$$

$$= a_o \frac{\sin(\psi_{o,-}^\pm)}{u\sqrt{1 - (u_o/u)^2 \sin^2(\psi_{o,-}^\pm)}}. \tag{51}$$

For convenience, we define

$$P(\psi_{o,-}^\pm) \triangleq \frac{(u_o/u)\cos(\psi_{o,-}^\pm)}{\sqrt{1 - (u_o/u)^2 \sin^2(\psi_{o,-}^\pm)}}, \tag{52a}$$

$$Q(\psi_{o,-}^\pm) \triangleq \frac{\sin(\psi_{o,-}^\pm)}{u\sqrt{1 - (u_o/u)^2 \sin^2(\psi_{o,-}^\pm)}}. \tag{52b}$$

Finally, we find the derivative of $\gamma^\pm$ as

$$\frac{d\gamma^\pm}{dt} = \pm r \pm r_o P(\psi_{o,-}^\pm) + \frac{\|\boldsymbol{v}_r\|}{d}(1 + P(\psi_{o,-}^\pm)) \tag{53}$$
$$(\pm\sin(\psi_r - \alpha) - \cos(\psi_r - \alpha)\tan(\beta)) \mp a_o Q(\psi_{o,-}^\pm).$$

Since the shortest distance to a conflict, γ, is defined as (21), we can write $\pm\sin(\psi_r - \alpha) = |\sin(\psi_r - \alpha)|$. Recall that the vehicle starts outside a conflict, i.e. satisfies (35). Since $|\tan(\psi_r - \alpha)| \geq \tan(\beta)$ the following must thus hold:

$$|\sin(\psi_r - \alpha)| - \cos(\psi_r - \alpha)\tan(\beta) \geq 0. \tag{54}$$

Moreover, (52a) and (52b) are bounded by Assumption 5:

$$P(\psi_{o,-}^\pm) \in \left[-\frac{u_o}{u}, \frac{u_o}{u}\right], \tag{55a}$$

$$Q(\psi_{o,-}^\pm) \in \left[-\frac{1}{\sqrt{u^2 - u_o^2}}, \frac{1}{\sqrt{u^2 - u_o^2}}\right]. \tag{55b}$$

Since $u > u_o$, then $|P(\psi_{o,-}^\pm)| < 1$. Hence, (53) can be reduced to

$$\frac{d\gamma^\pm}{dt} \geq \pm r \pm r_o P(\psi_{o,-}^\pm) \mp a_o Q(\psi_{o,-}^\pm). \tag{56}$$

From (56) we can formulate the following lower bound on the vehicle's required turning rate, in order to compensate for the obstacle's maximum turning rate, forward acceleration and speed:

$$r_{\max} \geq r_{o,\max}\frac{u_{o,\max}}{u} + \frac{a_{o,\max}}{\sqrt{u^2 - u_{o,\max}^2}}. \tag{57}$$

If the vehicle satisfies (57), then a continuous control input satisfying (37) also ensures that

$$\frac{d\gamma(t)}{dt} \geq 0, \quad \forall t \geq t_0, \tag{58}$$

meaning that the shortest angular distance to a conflict is either constant or increasing with time. Hence,

$$|\psi_r(t) - \alpha(t)| \geq \beta(t), \quad \forall t \geq t_0, \tag{59}$$

which implies that

$$d(t) - R_o \geq d_\epsilon, \quad \forall t \geq t_0, \tag{60}$$

by Lemma 2. ∎

The result of Theorem 1 agrees with intuition. If the vehicle is able to turn away from the obstacle faster than the obstacle can turn and accelerate towards it, then the vehicle will be able to escape the obstacle by turning in the opposite direction. Theorem 1 is useful because it proves that the vehicle will be able to maintain at least a safety distance to the obstacle at all times, provided $d_{\text{threshold}}$ is chosen large enough for the vehicle to turn out of any conflict before the obstacle comes within the safety distance. We will use this fact to prove the final theorem of the paper, where we require the following assumption to hold:

Assumption 6: The vehicle's maximum heading rate $r_{\max} > 0$ satisfies

$$r_{\max} \geq r_{o,\max}\frac{u_{o,\max}}{u} + \frac{a_{o,\max}}{\sqrt{u^2 - u_{o,\max}^2}}. \tag{61}$$

Theorem 2: Consider an obstacle described by (3) and a vehicle described by (1). If Assumption 1-6 hold, the vehicle follows the guidance law (8) with the heading controller (10), the switching rules (15)-(16), and the turning rules (23)-(25), then the vehicle will reach the target position $\boldsymbol{p}_t$ while maintaining a distance to the obstacle satisfying

$$d(t) - R_o \geq d_\epsilon, \quad \forall t \in [t_0, t_f], \tag{62}$$

where t_f is the time of arrival at $\boldsymbol{p}_t$, provided the vehicle and the obstacle initially are separated by a distance:

$$d(t_0) \geq R_o + d_\epsilon + \frac{2u + \pi u_{o,\max}}{r_{\max}}. \tag{63}$$

Proof: Let the vehicle enter CA mode at a time $t_1 \geq t_0$ as the distance satisfies $d(t_1) = d_{\text{threshold}}$. In order to satisfy condition (62) the vehicle must be able obtain a safe heading before the obstacle is closer than the safety distance, d_ϵ. To achieve this, the threshold distance should be above a lower bound, and it is shown in [14] that this minimum value is

$$d_{\min} \triangleq R_o + d_\epsilon + \frac{2u + \pi u_{o,\max}}{r_{\max}}. \tag{64}$$

As long as $d_{\text{threshold}} \geq d_{\min}$, and the vehicle and the obstacle are separated by a distance $d(t_0) \geq d_{\min}$, the vehicle will reach a safe heading satisfying

$$|\psi_r(t) - \alpha(t)| \geq \beta(t), \tag{65}$$

before the obstacle is within the safety distance of the vehicle. Since the vehicle follows the turning rule (24) until it exits collision avoidance mode at a time $t_2 > t_1$, the vehicle will maintain a heading angle satisfying (65), and keep a distance to the obstacle satisfying $d(t) - R_o \geq d_\epsilon$, $\forall t \in [t_0, t_2]$, by Theorem 1.

Since the obstacle can turn towards the vehicle after it exits CA mode, causing the current velocity to become unsafe, the vehicle has the possibility of re-entering CA mode. If the distance between the vehicle and the obstacle does not satisfy $d(t) = d_{\text{threshold}}$ at this point, the vehicle will immediately
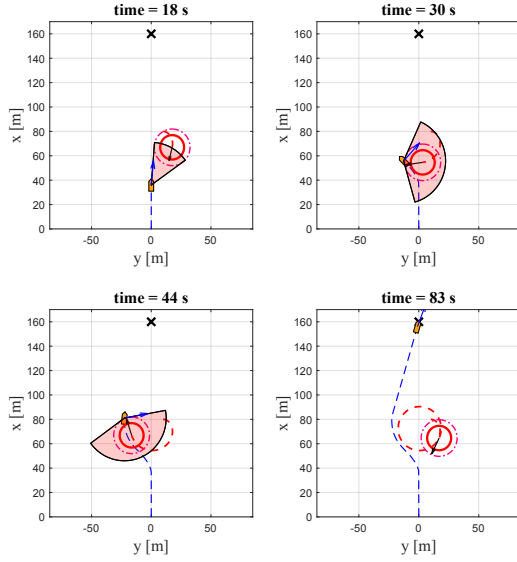
Fig. 3: The first scenario. The vehicle is the orange polygon and the obstacle is the red circle. The magenta circle represents the radius $R_{o|\epsilon}$. The obstacle and vehicle trajectories are the red and blue dashed lines, respectively. The target position, $\boldsymbol{p}_t$, is marked as an 'X'. The blue arrow represents $\boldsymbol{v}_{dgr}$, and the red cone represents $\mathcal{CC}_{o|\epsilon}$ with length $d_{threshold}$.

turn away from the conflict by the turning rule (25), ensuring that the vehicle cannot enter a conflict, i.e. satisfies (65) at all times. Hence, by Theorem 1 the vehicle will satisfy

$$d(t) - R_o \geq d_\epsilon, \ \forall t \in [t_0, t_f], \tag{66}$$

where t_f is the time of arrival at $\boldsymbol{p}_t$. Finally, since $u > u_{o,max}$ the vehicle will be able escape the obstacle at some point in time and proceed to the target $\boldsymbol{p}_t$. ∎

V. SIMULATIONS

This section presents numerical simulations of two scenarios where the vehicle avoids a moving obstacle by following the collision avoidance algorithm described in Section III. The vehicle is modeled as a unicycle (1) with constant forward speed equal to $u = 2$ m/s, and maximum turning rate $r_{max} = 0.5$ rad/s in both scenarios. The target position is chosen as $\boldsymbol{p}_t = [160, 0]^\top$ m. The minimum safety distance is set to $d_\epsilon = 5$ m, and the angular safety distance to $\epsilon = 10°$. The acceptance distance is chosen as $d_a = 4$ m. The obstacle is modeled as the nonholonomic vehicle (3) with radius $R_o = 10$ m.

In the first scenario, the obstacle turns in a clockwise circle while increasing its forwards speed, with constant turning rate equal to $r_o = r_{o,max} = 0.1$ rad/s and acceleration equal to $a_o = a_{o,max} = 0.05$ m/s². The obstacle's initial speed is $u_o(t_0) = 0.5$ m/s and its maximum speed is $u_{o,max} = 1.8$ m/s. The minimum threshold distance of Theorem 2 is computed as $d_{min} \approx 34.3$ m, and we choose $d_{threshold} = 35$ m. Assumption 6 holds with the presented parameters, verified by direct calculation.

The trajectories of the vehicle and the obstacle during the collision avoidance scenario are plotted at four different
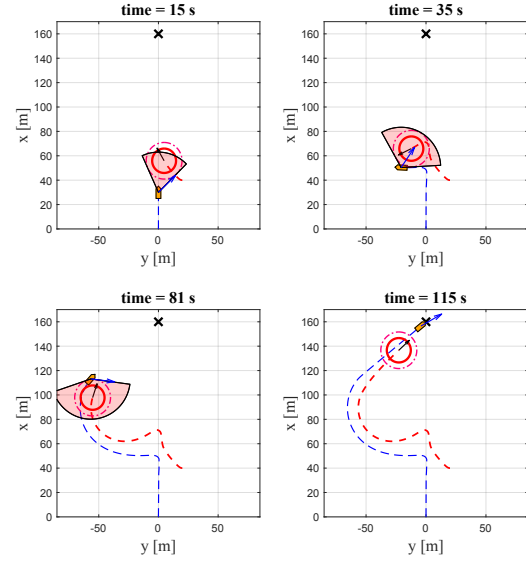

Fig. 4: The second scenario.

moments in time, in Figure 3. The relative guidance velocity, $\boldsymbol{v}_{dgr}(t) \triangleq \boldsymbol{v}_{dg}(t) - \boldsymbol{v}_o(t)$, is included in order to demonstrate when the vehicle enters and exits CA mode. It can be seen in the top left plot that the vehicle enters CA mode at $t = 18$ s, as $d(t) = d_{threshold}$. The vehicle turns left according to the turning rule (23), aiming to pass on the rear side of the obstacle. However, the obstacle turns and accelerates directly towards the vehicle, making the vehicle pass in front of it instead, seen in the top right plot. At $t = 44$ s the relative guidance velocity becomes safe, seen in the bottom left plot. The vehicle can then proceed to the target, which is finally reached at $t = 83$ s, seen in the bottom right plot of Figure 3. To verify that condition (7) holds, the distance between the vehicle and the obstacle, $d(t) - R_o$, has been plotted in Figure 5a, together with the threshold distance and the safety distance. Hence, the simulation result supports the theoretical result of Theorem 2.

In the second scenario, the obstacle follows the heading references generated by a constant bearing (CB) guidance law [15], with the vehicle position as the target, in order to purposely collide with the vehicle. To follow the heading references, the obstacle employs the same kinematic controller as the vehicle, defined in (10). Rather then pursuing the target, the CB guidance scheme accounts for the target's velocity vector in order to generate a direct collision course. The obstacle has a constant forward speed equal to $u_o = 1.5$ m/s, and maximum turning rate equal to $r_{o,max} = 0.4$ rad/s. We calculate $d_{min} \approx 32.4$ m, and choose $d_{threshold} = 33$ m. Assumption 6 is satisfied with the specified parameters.

Trajectories of the vehicle and the obstacle are plotted in Figure 4. The obstacle can be seen to cut in front of the vehicle in order to cause a collision, forcing the vehicle to enter CA mode at $t = 15$ s, in the top left plot. The vehicle enters CA mode as $d(t) < d_{threshold}$, and turns left according to turning rule (25), seen in the top right plot. The obstacle continues to block the vehicle's path as the vehicle attempts
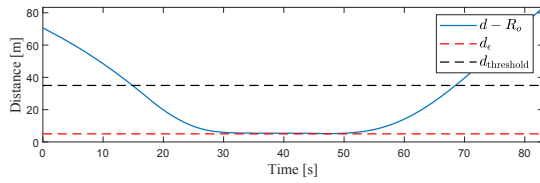
(a) Distance, $d(t) - R_o$, during the first simulation.
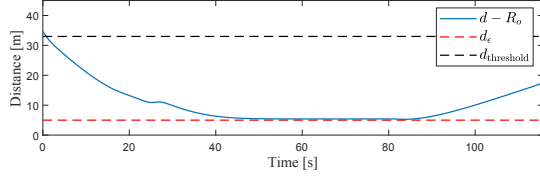
(b) Distance, $d(t) - R_o$, during the second simulation.

Fig. 5: Distance to the obstacle during both simulations.

to maneuver around the obstacle. Still, the vehicle manages to keep the required distance from the obstacle at all times by following the CA algorithm, verified by Figure 5b. The vehicle finally exits CA mode at $t = 81$ s and proceeds to the target, seen in the bottom two plots of Figure 4. Hence, we can conclude that the simulation result supports the theoretical result of Theorem 2.

VI. CONCLUSIONS AND FUTURE WORK

This paper has presented a mathematical analysis of the velocity obstacle algorithm applied to a nonholonomic vehicle for reactive collision avoidance of a moving obstacle. The algorithm is based on mapping the obstacle to the velocity space as a set of unsafe velocities, called the velocity obstacle, and the vehicle avoids the obstacle by maintaining velocities outside of this set. The main contribution of this paper is a theoretical analysis of the performance of the algorithm when applied to a vehicle in a collision avoidance scenario. The vehicle is restricted to maintain a constant forward speed, and is subject to nonholonomic constraints. Despite this, the analysis shows that the vehicle can safely avoid a moving obstacle, even in the case where the obstacle is able to turn and accelerate towards the vehicle. This is in contrast to the original formulation of velocity obstacles, which both assumes that the obstacle maintains a constant velocity, and does not deal well with vehicles with restricted forward speed and nonholonomic constraints.

Although safety analyses have been presented for the multi-agent scenario, we here analyze the algorithm without any assumptions on the decision-making of the obstacle, and allow for fully non-cooperative behaviour. In the extreme case, this means that the obstacle could aim to collide with the vehicle. Still, we are able to guarantee vehicle safety in any scenario under the mild assumption that the vehicle's speed is lower bounded by the obstacle speed, and by requiring the vehicle's turning rate to satisfy a lower bound. This was demonstrated through simulations where the obstacle actively sought to collide with the vehicle.

In this paper, we have examined scenarios with a circular obstacle. This is not a requirement of the algorithm; if the obstacle shape is non-circular, the collision cone may be computed to fit the exact shape of the obstacle by substituting the circular domain, $\mathcal{D}_o$, with any shaped domain, $\mathcal{D}$. However, the performance of the algorithm in such cases remains to be analysed and is a topic of future research. Other topics concern the issue of avoiding multiple moving obstacles, and applying the algorithm to nonholonomic vehicles capable of acceleration/deceleration. Analysis of such scenarios is inherently more complex and remains a subject for future work.

REFERENCES

[1] P. Fiorini and Z. Shiller, "Motion planning in dynamic environments using velocity obstacles," *The International Journal of Robotics Research*, vol. 17, no. 7, pp. 760–772, 1998.
[2] E. Owen and L. Montano, "Motion planning in dynamic environments using the velocity space," in *Proc. IEEE/RSJ International Conference on Intelligent Robots and Systems*, pp. 2833–2838, 2005.
[3] D. Wilkie, J. van den Berg, and D. Manocha, "Generalized velocity obstacles," in *Proc. IEEE/RSJ International Conference on Intelligent Robots and Systems*, pp. 5573–5578, 2009.
[4] Y. Kuwata, M. Wolf, D. Zarzhitsky, and T. Huntsberger, "Safe maritime autonomous navigation with colregs, using velocity obstacles," *IEEE Journal of Oceanic Engineering*, vol. 39, pp. 110–119, 2014.
[5] Y. Huang, L. Chen, and P. Gelder, "Generalized velocity obstacle algorithm for preventing ship collisions at sea," *Ocean Engineering*, pp. 142–156, 2019.
[6] J. van den Berg, J. Snape, S. J. Guy, and D. Manocha, "Reciprocal collision avoidance with acceleration-velocity obstacles," in *Proc. IEEE International Conference on Robotics and Automation*, pp. 3475–3482, 2011.
[7] F. Large, S. Sckhavat, Z. Shiller, and C. Laugier, "Using non-linear velocity obstacles to plan motions in a dynamic environment," in *Proc. 7th International Conference on Control, Automation, Robotics and Vision*, pp. 734–739, 2002.
[8] Y. I. Jenie, E.-J. V. Kampen, C. C. de Visser, J. Ellerbroek, and J. M. Hoekstra, "Three-dimensional velocity obstacle method for uncoordinated avoidance maneuvers of unmanned aerial vehicles," *Journal of Guidance, Control, and Dynamics*, vol. 39, no. 10, pp. 2312 – 2323, 2016.
[9] Y. I. Jenie, E.-J. V. Kampen, C. C. de Visser, J. Ellerbroek, and J. M. Hoekstra, "Three-dimensional velocity obstacle method for UAV deconflicting maneuvers," in *Proc. AIAA Guidance, Navigation, and Control Conference*, 2015.
[10] E. Lalish, K. A. Morgansen, and T. Tsukamaki, "Decentralized reactive collision avoidance for multiple unicycle-type vehicles," in *Proc. 47th IEEE Conference on Decision and Control*, pp. 5055 – 5061, 2008.
[11] E. Lalish and K. A. Morgansen, "Distributed reactive collision avoidance," *Autonomous Robots*, vol. 32, pp. 207 – 226, 2012.
[12] J. van den Berg, M. Lin, and D. Manocha, "Reciprocal velocity obstacles for real-time multi-agent navigation," in *Proc. IEEE International Conference on Robotics and Automation,*, pp. 1928–1935, 2008.
[13] J. Snape, J. van den Berg, S. Guy, and D. Manocha, "The hybrid reciprocal velocity obstacle," *IEEE Transactions on Robotics*, vol. 27, no. 4, pp. 696–706, 2011.
[14] M. S. Wiig, K. Y. Pettersen, and A. V. Savkin, "A reactive collision avoidance algorithm for nonholonomic vehicles," in *Proc. IEEE Conference on Control Technology and Applications*, pp. 1776–1783, 2017.
[15] T. I. Fossen, *Handbook of Marine Craft Hydrodynamics and Motion Control*. John Wiley & Sons, 2011.